

Analysis of impulsive biological noise due to snapping shrimp as a point process in time

Matthew W. Legg
Maritime Operations Division
Defence Science and Technology Organisation
Rockingham, Western Australia 6958
Email: matthew.legg@dsto.defence.gov.au

Alec J. Duncan
Centre for Marine Science and Technology
Curtin University of Technology
Bentley, Western Australia 6845
Email: a.duncan@cmst.curtin.edu.au

Anthony Zaknich
Centre for Marine Science and Technology
Curtin University of Technology
Bentley, Western Australia 6168
Email: tonko@ieee.org

Michael V. Greening
Maritime Operations Division
Defence Science and Technology Organisation
Edinburgh, South Australia 5111
Email: mike.greening@dsto.defence.gov.au

Abstract—Impulsive biological noise produced by snapping shrimp provides an important contribution to the ambient acoustic noise in warm, coastal waters. The challenge is to understand and model the properties of shrimp noise to reduce its impact on sonar and underwater acoustic telemetry systems. Shrimp snaps are impulsive events occurring apparently at random. The short duration of each snap allows these events to be modeled as a point process in time. Point processes are used to model many naturally occurring phenomena including neuron firings, seismic events, radioactive decay, lightning discharges and shot noise in semiconductors. In this paper, point process analysis techniques are applied to real shrimp noise. Inter-snap interval histogram and Fano-factor analysis provide strong evidence that the snaps are not homogeneous Poisson distributed in time. Further analysis based on the rate function suggests that the data may be more appropriately modeled by a doubly stochastic Poisson process.

is known that shrimp noise is non-Gaussian [7], and there is evidence for snaps to exhibit bursting in time [2].

In this paper we test the assumption that shrimp noise samples are independent of each other. We start by applying a simple test for homogeneous Poisson statistics based on the distribution of intervals. Upon finding that the intervals are not necessarily distributed as expected, a more revealing analysis is conducted using the Fano-factor (or Index of Dispersion of Counts). The Fano-factor analysis reveals that the snaps are more clustered than expected for a homogeneous Poisson process. We investigate further by assuming the shrimp snaps form a doubly-stochastic process, and find that an Ornstein-Uhlenbeck driven doubly-stochastic Poisson process can be used to model medium time clustering in the shrimp noise.

I. INTRODUCTION

Snapping shrimp are commonly found in warm shallow waters, particularly in reefs or near structures such as piers, wharfs and rock walls, or where debris covers the sea floor. Although only a few centimeters in length, the noise they produce by creating cavitation bubbles with their enlarged claw [1] makes a significant contribution to underwater acoustic ambient noise [2], [3], [4]. The snaps are highly impulsive, with peak-to-peak source levels of up to 189 dB re 1 μ Pa at 1 m [5], and are broadband with frequencies ranging from 600 Hz up to 250 kHz.

Understanding how shrimp noise contributes to the overall ambient noise is important for sonar and acoustic telemetry systems. Statistical models of the ambient noise are particularly useful because of their direct application in optimized signal processing algorithms [6].

In many signal processing algorithms noise is assumed to be independent and identically distributed (i.i.d), and this is often coupled with the assumption that the distribution will be Gaussian by virtue of the Central Limit theorem. However, it

II. EVENT TIMESERIES

A. Shrimp noise data

Ambient noise measurements were conducted in Cockburn Sound, Western Australia. A TC4034-3 reference hydrophone was suspended from a pontoon at a depth of 5 m and sampled at 500 kHz. Pre-whitening filters were not used in order to preserve as much of the original phase information as possible. The measurements were conducted at times when the weather was fine and sea states as low as possible. Shipping and small boat activity was common during measurements, and at times dolphins came within 100 m of the hydrophone. A representative time series was selected from the measurements.

Two other time series were sourced from measurements taken near Feather Reef (Queensland, Australia) and Seal Island (Western Australia). These measurements were made using DAT recorders and have low bandwidth relative to the Cockburn Sound measurements. Details of these measurements can be found in [8].

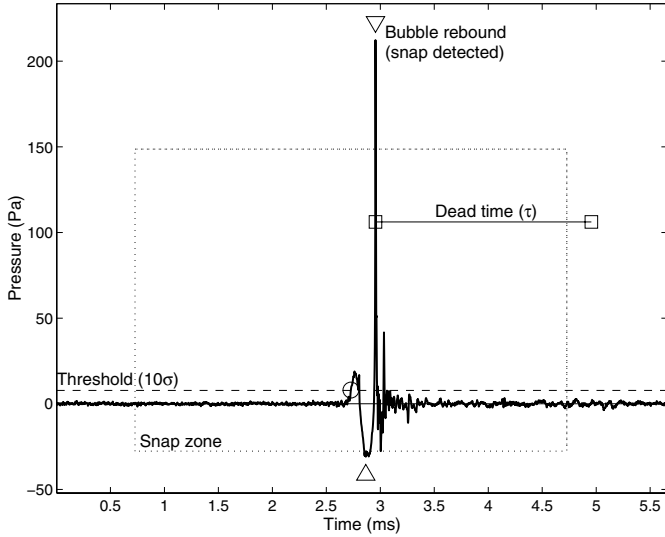


Fig. 1. A graphical representation of snap detection. The threshold (dashed horizontal line at 10σ), threshold exceedance (circle), snap zone (dashed box), detection points (triangles) and dead-time (square ended bar) are shown.

B. Conversion to event time series

The ambient noise time series were converted to event time series by a process of filtering and threshold detection. High-pass filtering with a linear-phase 1 kHz filter was applied to remove unnecessary low frequency components. A threshold was set at 10 standard deviations (σ) above zero pressure to keep false alarms low. Samples that exceeded the threshold had a *snap zone* identified about them, as shown in Fig. 1, and the maximum amplitude in the zone declared as an event. A fixed length dead time was inserted after each event detection to allow any oscillations following the snap impulse to relax to levels below the threshold. False detections were identified by visual inspection and removed.

III. STATISTICAL METHODS

A. Homogeneous and doubly-stochastic Poisson processes

The homogeneous Poisson process (HPP) is a mathematical concept used to describe a completely random series of events [9]. When considering events occurring in time, the process has the following descriptive properties (for a more mathematical treatment see [9], [10] or [11]):

- 1) There is no trend in the series;
- 2) Two or more events cannot occur at exactly the same instant of time and;
- 3) What happens in one time window is completely independent of what happens in any other non-overlapping time window, irrespective of the window length or the interval of time between them.

Two important distributions that arise from a Poisson process are the distribution of the number of events (N_t) in a given time window, and the distribution of time intervals

(Δ) between events. For a homogeneous Poisson process the probability density of N_t is defined by

$$\Pr\{N_t = x\} = \frac{(\lambda t)^x \exp(-\lambda t)}{x!} \quad (1)$$

and the mean and variance are equal

$$E[x] = \text{var}(x) = \lambda t \quad (2)$$

where $E[\cdot]$ and $\text{var}(\cdot)$ are respectively expectation and variance operators. The name *rate of occurrence* is given to the parameter λ because N_t/t converges in probability to λ in the limit $t \rightarrow \infty$ [9]. For the same process, the distribution of Δ is

$$F(\Delta) = 1 - \exp(-\lambda\Delta) \quad (3)$$

so that the probability density of intervals is

$$f(\Delta) = \frac{\partial F(\Delta)}{\partial \Delta} = \lambda \exp(-\lambda\Delta) \quad (4)$$

which is an exponential distribution. This density of intervals provides the basis for the simple HPP test using inter-snap interval histograms.

A process is doubly stochastic if $\lambda(t)$ is not a deterministic function but rather a realization of a stationary, time varying stochastic process $\{\Lambda(t)\}$ [9].

B. Inter-snap interval histograms

A simple test for the homogeneous Poisson process is to compare the inter-snap interval histogram (IIH) with the theoretical distribution. The theoretical distribution for events detected using a dead-time is the dead-time modified exponential density function [12]

$$f(\Delta) = \lambda \exp(-\lambda(\Delta - \tau)). \quad (5)$$

Testing can be conducted using visual and statistical methods. For visual comparison the IIH was computed using empirical probability density functions [13]. Left and right censure corrections were applied to account for the dead-time, and the duration limit of the event time series. These results are presented in the next section.

Test statistics were computed to provide an objective test to use in conjunction with visual comparison. Kolmogorov-Smirnov (D), Cramér-von Mises (W^2), and Anderson-Darling (A^2) statistics were computed according to [14]. Of these statistics, the Anderson-Darling (A^2) gave the most consistent result. The consistency of A^2 was attributed to the information contained in the tail of the distributions. The statistic was computed using

$$A^2 = -n - \frac{1}{n} \left(\sum_{k=1}^n \{(2k-1)(\ln(Z_k) + \ln(1-Z_{n+1-k}))\} \right) \quad (6)$$

where n was the number of observations, and the Z_k values were ordered (ascending) observations transformed using

$$Z_k = 1 - \exp(-\lambda(\Delta_k - \tau)) \quad (7)$$

where parameter τ is the known dead-time (in seconds) and λ is estimated from the observations using the method of moments.

C. Fano-factor analysis

The Fano-factor (or Index of Dispersion of Counts) is defined as the variance to mean ratio of the counting process N_ϖ [15], [16]. An equivalent definition, that is useful for analytic solutions, is the ratio of the variance-time function to its value for a homogeneous Poisson process [9]. In these definitions time refers to *counting time* (ϖ). The counting time is the time over which the process is observed and the events counted, sometimes referred to as a counting window or window of observation. For all Fano-factor computations the windows of observation were non overlapping.

For a homogeneous Poisson process the variance and mean are equal and independent of time. Using the variance to mean ratio definition, the Fano-factor (FF) is equal to

$$FF_{hpp}(\varpi) = \frac{\text{var}(N_\varpi)}{E[N_\varpi]} = 1 \quad (8)$$

where the subscript *hpp* indicates that the result is for a homogeneous Poisson process only.

For the doubly-stochastic Poisson process the variance (V) varies with counting time (ϖ) according to the variance-time function

$$V(\varpi) = \bar{\lambda}\varpi + 2\bar{\sigma}^2 \int_0^\varpi (\varpi - u)\rho(u) du \quad (9)$$

where $\bar{\lambda}$, $\bar{\sigma}^2$ and $\rho(u)$ are respectively the mean, variance and autocorrelation function of the stochastic rate process $\{\Lambda(t)\}$ that drives the DSPP. The Fano-factor for a doubly-stochastic Poisson process can then be found using the variance-time function definition

$$FF_{dspp}(\varpi) = \frac{V(\varpi)}{\bar{\lambda}\varpi} = 1 + \frac{2\bar{\sigma}^2}{\bar{\lambda}\varpi} \int_0^\varpi (\varpi - u)\rho(u) du. \quad (10)$$

Empirical estimates of the Fano-factor were computed as follows. For a fixed duration (ϖ) window the number of counts in each window forms the values c_k and these values are used to compute the Fano-factor for that particular window duration. The computation is the ratio of the variance of c_k values divided by the mean c_k , thus

$$FF(\varpi) = \frac{\text{var}\{c_1, c_2, \dots, c_n\}_\varpi}{E\{c_1, c_2, \dots, c_n\}_\varpi} \quad (11)$$

where there are a unique set of $c_k = \{c_1, c_2, \dots, c_n\}$ values for each window duration, indicated using the subscript ϖ at the end of the set. Statistical fluctuations exist in Fano-factor estimates that become more variable with increasing counting time. The increase in variability is a direct consequence of truncation of the period of observation and is present for all empirical results, including the HPP result. Significance levels cannot be computed for the Fano-factor because its distribution is not known exactly [9]. Instead, guide levels are computed by shuffling (randomly permuting) the order of intervals as suggested by Lowen and Teich [17]. The shuffling technique destroys any correlation between events but at the same time preserves the distribution of inter-snap intervals. By conducting a number of shuffles of the data and recomputing the Fano-factors the mean and standard deviation of the shuffled data

can be used as a guide for normal fluctuation. Deviations above the upper guide level indicate clustering of the events, referred to as super-Poisson; conversely deviations below the lower guide level indicate anti-clustering (or increased orderliness) and are referred to as sub-Poisson.

D. Intensity process and the rate function

For a doubly-stochastic Poisson process, the rate of occurrence is a function of time, $\lambda(t)$, and is a realisation of a stationary stochastic process $\{\Lambda(t)\}$ [9]. It is, therefore, the properties of $\{\Lambda(t)\}$ that are of interest. For real processes it is difficult to estimate the properties of $\{\Lambda(t)\}$. The difficulty arises because the observed events are a realization of a doubly-stochastic Poisson process; they are not a realization of $\{\Lambda(t)\}$. For this reason the properties of $\{\Lambda(t)\}$ are estimated using smoothed rates computed as a function of time. We call the smooth, time varying rates the *rate function*, $R(t)$. When computing $R(t)$ using window-based estimation, the time duration of the window becomes important. The window needs to be concurrently large enough to allow reasonable estimates of rate, and small enough to capture important variations with time. Optimum window estimators can be formed if the autocorrelation function ($\rho(u)$) of the intensity process is known [18], [10]. If the autocorrelation function is not known then a simple histogram estimator can be used [10].

For an Ornstein-Uhlenbeck (O-U) process the distribution of intensities is Gaussian, with mean $\bar{\lambda}$ and variance $\bar{\sigma}^2$. The intensities are correlated in time, with an exponentially decaying autocorrelation function

$$\rho(u) = \exp(-u/l) \quad (12)$$

where l is a measure of correlation time (in seconds). We estimate the parameters $\bar{\lambda}$ and $\bar{\sigma}^2$ from the rate function $R(t)$ using the simple histogram method with a reasonably large window duration. The correlation time (l) is then computed by assuming that the shrimp snap events are exponentially correlated. Under this assumption the Fano-factor curve will have a finite asymptote in the limit of infinite counting time ($\varpi \rightarrow \infty$) given by

$$FF_{ou}(\infty) = 1 + \frac{2\bar{\sigma}^2 l}{\bar{\lambda}} \quad (13)$$

so that l can be estimated given $FF_{ou}(\infty)$. The value of $FF_{ou}(\infty)$ was estimated as the average value of Fano-factors over the upper quarter of the counting times.

IV. RESULTS & DISCUSSION

A. Inter-snap interval histograms

Inter-snap interval histograms were computed using 100 bins evenly spaced across the range of intervals. For each individual data set an estimate of λ was computed using the method of moments [8] and used to produce the theoretical curve (5). The results are shown using semilogarithmic plots in Fig. 2 so that the exponential distribution lies on a straight line. Visual judgments between the histogram (point markers) and theoretical curve (solid line) are recorded in Table I.

TABLE I
IIH TEST RESULTS

Data	Visual	A^2	95% test ($A^2 < 1.321$)	accept HPP
HPP	pass	1.00	pass	yes
FR	fail	22.9	fail	no
CS	pass	0.44	pass	yes
SEAL	fail	107	fail	no

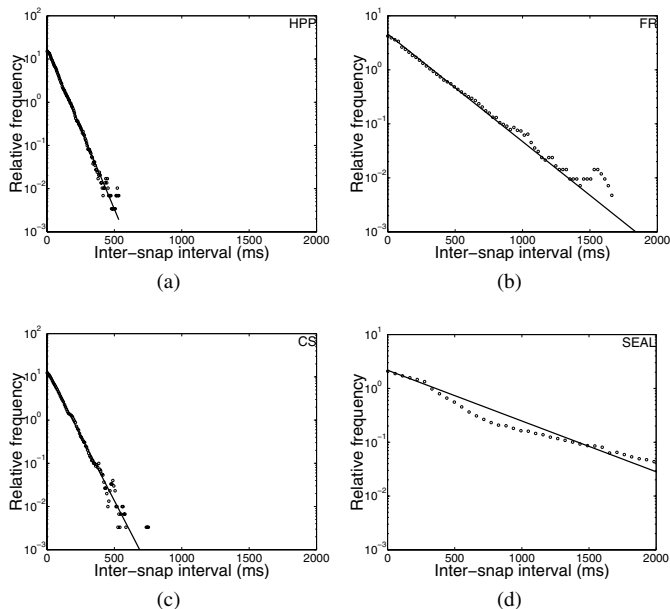


Fig. 2. Inter-snap interval histograms computed from simulated HPP (a), Feather Reef (b), Cockburn Sound (c) and Seal Island (d) data (point markers) plotted along with a theoretical dead-time modified exponential curve (solid line).

Statistical testing using the Anderson-Darling statistic (6) was conducted at the 95% confidence level. The decision value for this level of confidence was 1.321 (taken from tables in [14]). Corrections were applied for unknown scaling parameter $\bar{\lambda}$. The test results are recorded in Table I.

Decisions based on combined visual and statistical IIH tests showed that the simulated HPP and Cockburn Sound processes were consistent with a homogeneous Poisson process, and that the Feather Reef and Seal Island processes were not consistent with a homogeneous Poisson process. Although the Cockburn Sound data passes the HPP test based on histograms, a more sophisticated Fano-factor analysis (see Section IV-C) reveals evidence of super-Poisson behavior.

B. Rate functions

Rate functions were computed using a simple histogram estimator with a five second window duration. Results for Feather Reef and Seal Island data are shown in Fig. 3. Cockburn Sound results are not shown because they are very similar to the Feather Reef results. In the figures the rate as a function of time is plotted along with a histogram of the samples. A Gaussian fit to the histogram is also shown.

The Seal Island rate function reveals an abrupt change near

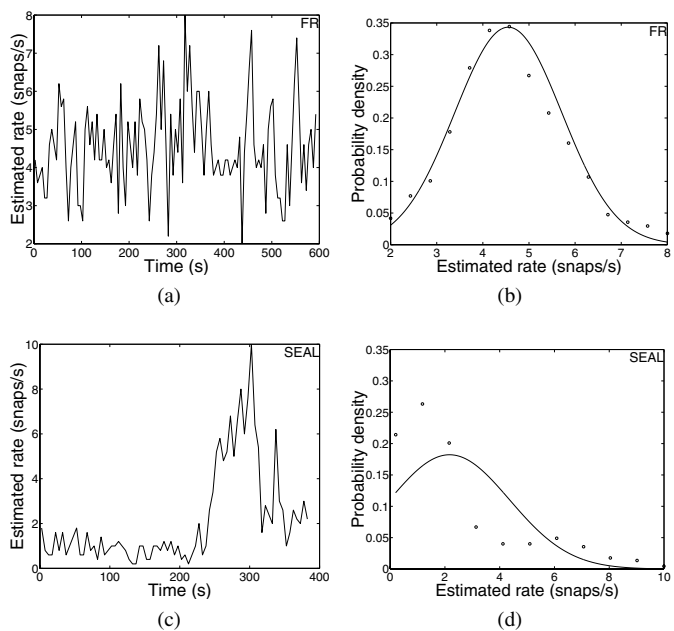


Fig. 3. Rate functions for Feather Reef (a) and Seal Island (c) computed using the simple histogram method. A histogram of rates (circles) and a Gaussian fit (solid line) are shown for Feather Reef (b) and Seal Island (d).

230 s resulting in two peaks in the histogram and a poor fit to a Gaussian. When data contains such bursts in rate, the O-U model is clearly inappropriate. In contrast, the Feather Reef rates are modeled well by a Gaussian distribution. The O-U model may be suitable for the Feather Reef intensity process if, in addition to being Gaussian distributed, intensities are exponentially correlated with time.

In cases where the real shrimp noise is approximately homogeneous, the variance in the rate function will tend to zero and the O-U intensity process will reduce to a constant. Under these conditions the O-U driven DSPP will reduce to a HPP and therefore continue to model the process correctly.

C. Fano-factor analysis

Empirical Fano-factor curves were computed as a function of counting time using (11). The minimum counting time was set equal to the dead-time, which was 0.001 s in all cases. The maximum counting time was set at 1/10 the duration of the time series to ensure that the computation of variance and mean had at least 10 sample points. Counting times were logarithmically spaced between the minimum and maximum values using a log base of 1.05. When referring to counting times we will use the term *short time* for times less than a second, and the term *medium time* for times greater than a second, and less than 60 seconds.

The empirical Fano-factors for a simulated HPP data set (circle markers) are shown in Fig. 4. Upper and lower guide levels (solid lines) were computed using 100 shuffles of the data and set at two standard deviations beyond the mean. The guide levels bound 95% of the Fano-factors, indicating that the process is HPP over all counting times. At short counting times the value of the Fano-factors tend to a value slightly less

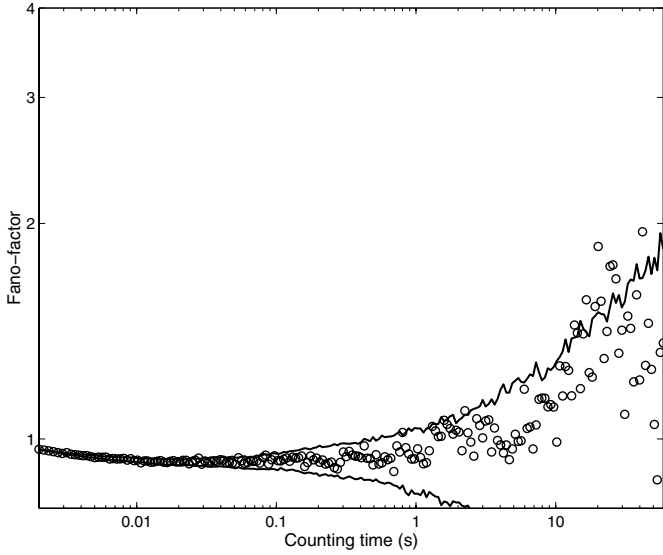


Fig. 4. Fano-factor versus counting time for simulated HPP events (circles), with positive and negative guide levels (solid lines).

than unity. The reason that the values do not tend exactly to unity is because dead-time was used in the detection process [19]. Inclusion of dead-time in the detection process reduces the variance, but not the mean, of the counts so that the count variance to mean ratio is less than unity. At longer counting times statistical fluctuations become more variable for the empirical Fano-factor because fewer samples (counting windows) are available for estimating the count mean and variance. The guide levels reflect this variability through increasing separation with increasing counting time. Empirical results above the upper guide level indicate super-Poisson behavior and results below the lower guide level indicate sub-Poisson behavior. Results between the guide levels indicate HPP behavior.

Fig. 5 shows empirical Fano-factor results computed from the Cockburn Sound data. Cross markers show the results when processing was applied to all events detected by the automatic (threshold) detector. There are two distinct sections in these results: a short time rise and plateau, and an ascent for medium counting times. The short time rise and plateau was considered to be a valid super-Poisson result, most likely caused by surface reflected snap replicas being included as events. To investigate further, the events were revisited using visual inspection and any surface reflected replicas removed to give a direct-path process. Fano-factor results for the direct-path process are shown in Fig. 5 using triangle markers. The short time rise and plateau are not evident in the direct-path results. An upper guide level (solid line) was computed using 100 shuffles of the direct-path results and set at two standard deviations above the mean. All of the direct-path results lie below the upper guide at short counting times. For medium counting times the direct-path result deviates above the guide levels, so the ascent for medium counting times remains. It

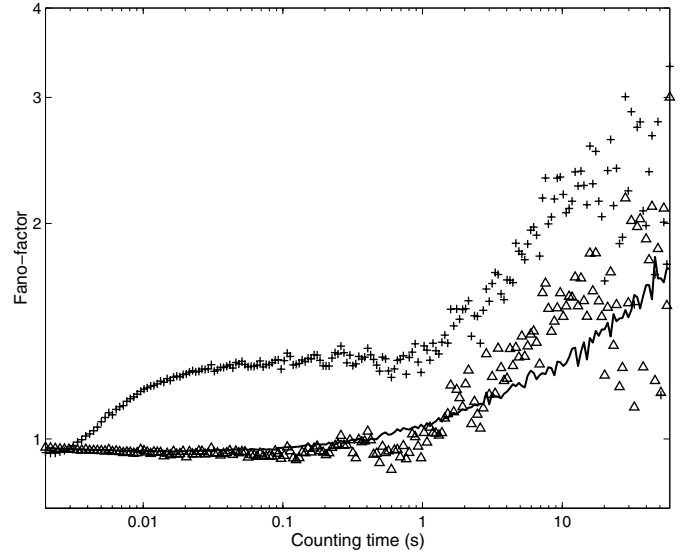


Fig. 5. Fano-factor versus counting time for Cockburn Sound with surface reflected events (cross markers) and with surface reflected events removed (triangle markers). The guide level shows normal fluctuation levels for the Cockburn Sound result with surface reflected events removed.

was concluded that the short time rise and plateau was caused by surface reflected snap replicas being included as events in the process.

Empirical Fano-factor results for the Feather Reef data are shown in Fig. 6 (triangle markers). A theoretical curve (solid line) for an O-U driven DSPP with parameters $\bar{\lambda} = 6.45$, $\bar{\sigma} = 1.27$ and $\tau = 3.67$, estimated using a nonlinear least squares regression fit of (10), with autocorrelation function (12), is also shown. Dead-time was not accounted for in the theoretical model, which explains the small offset between the theoretical curve and the dead-time corrected HPP result (dotted line) at short counting times. To test the effect of dead-time over medium counting times a simulated O-U driven DSPP event time series was generated and processed with and without dead-time detection. The difference between Fano-factors using the two processing methods was small relative to statistical fluctuations in the Fano-factors over medium counting times.

The Feather Reef results show super-Poisson deviations (clustering) for short and medium counting times. Short time clustering was due to surface reflected replicas included in the process, and is not modeled by the O-U driven doubly-stochastic Poisson process. Good agreement was found between the empirical Fano-factor curve and the O-U driven DSPP model at medium counting times. The model predicts a finite asymptote, shown in Fig. 6 using a long dashed line. A finite asymptote indicates that a process is not fractal [20]. Unfortunately, the asymptotic value cannot be confirmed for the empirical values because statistical fluctuations obscure the behavior of the Fano-factor curve at these counting times.

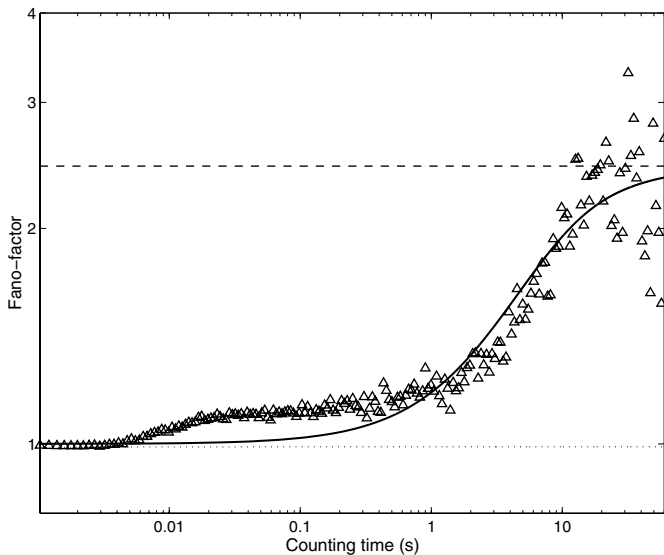


Fig. 6. Fano-factor versus counting time for Feather Reef events (triangle markers). A theoretical curve (solid line) shows the expected values for an O-U driven DSPP with parameters estimated from the Feather Reef data. The O-U driven DSPP asymptote for infinite counting time is shown using a long dashed line. The dotted line (near unity) shows the expected value for a dead-time modified homogeneous Poisson process.

V. CONCLUSION

We have presented a suite of techniques for analysis of point processes and demonstrated how they are applied to real snapping shrimp data. Inter-snap interval histogram analysis has been conducted with mixed success using visual and statistical tests. Rate function and Fano-factor analysis have been used to reveal more detail about the snapping process and has shown that real shrimp noise may be more clustered than expected over short and medium counting times. Short time clustering was caused by the inclusion of surface reflected events into the process. When snap rates were approximately Gaussian, the Ornstein-Uhlenbeck driven doubly-stochastic Poisson process was able to model medium time clustering. When clustering is minimal, the O-U driven DSPP reduces to a homogeneous Poisson process and therefore provides a more complete and appropriate model for describing snap events in snapping shrimp noise.

ACKNOWLEDGMENT

The authors would like to acknowledge Dave Matthews and Rob McCauley for providing respectively the Seal Island and Feather Reef data. We would like to thank Dave Matthews, Mark Savage and Rod MacLeod for their assistance with the Cockburn Sound measurements. Thanks also go to Derek Bertilone for his guidance and discussion on statistical analysis and the Fano-factor.

REFERENCES

- [1] M. Versluis, B. Schmitz, A. von der Heydt, and D. Lohse, "How snapping shrimp snap: through cavitating bubbles," *Science*, vol. 289, pp. 2114–2117, September 2000.
- [2] D. H. Cato and M. J. Bell, "Ultrasonic ambient noise in Australian shallow waters at frequencies up to 200kHz," Materials Research Laboratory, Australia, MRL Technical Report MRL-TR-91-23, February 1992.
- [3] E. O. Hulbert, "An underwater sound of natural origin," *J. Acoust. Soc. Am.*, vol. 14, no. 3, pp. 173–174, January 1943.
- [4] F. A. Everest, R. W. Young, and M. W. Johnson, "Acoustical characteristics of noise produced by snapping shrimp," *J. Acoust. Soc. Am.*, vol. 20, no. 2, pp. 137–142, March 1948.
- [5] W. W. L. Au and K. Banks, "The acoustics of the snapping shrimp *Synalpheus parneomeris* in Kaneohe Bay," *J. Acoust. Soc. Am.*, vol. 103, no. 1, pp. 41–47, January 1998.
- [6] M. A. Chitre, J. R. Potter, and S.-H. Ong, "Optimal and near-optimal signal detection in snapping shrimp dominated ambient noise," *IEEE J. Oceanic Eng.*, vol. 31, no. 2, pp. 497–503, April 2006.
- [7] P. A. Nielsen and J. B. Thomas, "A comparison of parametric and nonparametric detector performance levels in underwater noise," *J. Acoust. Soc. Am.*, vol. 87, no. 1, pp. 225–236, January 1990.
- [8] M. W. Legg, A. J. Duncan, A. Zaknich, and M. V. Greening, "An exploratory analysis of non-poisson temporal behaviour in snapping shrimp noise," in *Proceedings of Acoustics 2005*, November 2005, pp. 399–403.
- [9] D. R. Cox and P. A. W. Lewis, *The statistical analysis of series of events*, ser. Methuen's Monographs on Applied Probability and Statistics, M. S. Bartlett, Ed. London: Methuen & Co, Ltd, 1966.
- [10] D. L. Snyder and M. I. Miller, *Random point processes in time and space*, 2nd ed., ser. Springer Texts in Electrical Engineering, J. B. Thomas, Ed. New York: Springer, 1991.
- [11] R. V. Hogg and A. T. Craig, *Introduction to mathematical statistics*, 5th ed., R. W. Pirtle, Ed. New Jersey: Prentice Hall, 1995.
- [12] L. Ricciardi and F. Esposito, "On some distribution functions for non-linear switching elements with finite dead time," *Kybernetik*, vol. 3, pp. 148–152, 1966.
- [13] M. S. Waterman and D. E. Whiteman, "Estimation of probability densities by empirical density functions," *Int. J. Math. Educ. Sci. Technol.*, vol. 9, no. 2, pp. 127–137, 1978.
- [14] R. B. D'Agostino and M. A. Stephens, Eds., *Goodness of fit techniques*, ser. Statistics, textbooks and monographs. New York: Marcel Dekker, Inc., 1986, vol. 68.
- [15] M. C. Teich, R. G. Turcott, and R. M. Siegel, "Temporal correlation in cat striate-cortex neural spike trains," *IEEE Engineering in Medicine and Biology*, vol. 15, no. 5, pp. 79–87, September 1996.
- [16] U. Fano, "Ionization yield of radiations. ii. the fluctuations of the number of ions," *Physical Review*, vol. 72, no. 1, pp. 26–29, July 1947.
- [17] S. B. Lowen and M. C. Teich, "Auditory-nerve action potentials form a nonrenewal point process over short as well as long time scales," *J. Acoust. Soc. Am.*, vol. 92, no. 2, pp. 803–806, August 1992.
- [18] J. Virtamo, S. Aalto, and D. Down, "Window based estimation of the intensity of a doubly stochastic Poisson process," in *Proceedings of the International IFIP-IEEE Conference on Broadband Communications*, 1996, April 1996, pp. 294–305.
- [19] B. I. Cantor and M. C. Teich, "Dead-time-corrected photocounting distributions for laser radiation," *Journal of the Optical Society of America*, vol. 65, no. 7, pp. 786–791, July 1975.
- [20] S. B. Lowen and M. C. Teich, "The periodogram and Allan variance reveal fractal exponents greater than unity in auditory-nerve spike trains," *Journal of the Acoustical Society of America*, vol. 99, no. 6, pp. 3585–3591, June 1996.